

# FasR and FasL in colorectal cancer

MAGDALENA SZARYNSKA<sup>1</sup>, AGATA OLEJNICZAK<sup>1</sup>, PIOTR WIERZBICKI<sup>1</sup>,  
JAROSLAW KOBIELA<sup>2</sup>, DARIUSZ LASKI<sup>2</sup>, ZBIGNIEW SLEDZINSKI<sup>2</sup>,  
KRYSZTOF ADRYCH<sup>3</sup>, MAREK GUZEK<sup>3</sup> and ZBIGNIEW KMIEC<sup>1</sup>

<sup>1</sup>Department of Histology, Medical University of Gdansk, 80-210 Gdansk;  
Departments of <sup>2</sup>General, Endocrine and Transplant Surgery and  
<sup>3</sup>Hepatology and Gastroenterology, Medical University of Gdansk,  
Invasive Medicine Centre, 80-214 Gdansk, Poland

Received February 13, 2017; Accepted July 11, 2017

DOI: 10.3892/ijo.2017.4083

**Abstract.** Colorectal cancer (CRC) is one of the most common solid organ cancers prevalent worldwide causing, in spite of advancing therapeutic methodology, high rate of patient mortality, especially due to metastasis development. The cancer stem cell (CSC) theory of tumor growth indicates that CSCs within the tumor mass have great capacity to initiate and sustain tumor growth. Following the suggestion that Fas signaling can be engaged in apoptosis, tumor maintenance, senescence or DICE (death induced by CD95 or CD95L elimination), the attempts to broaden the knowledge concerning the relationships between CSCs features and FasR/FasL appeared to be necessary. The most important advantage of our study was the simultaneously analysis of CSCs from commonly used CRC lines (HCT116 and HT29) and tumor fragments collected from CRC patients. Moreover, the sphere-promoting expansion of CRC lines brought a specific three-dimensional specific environment for CSC exploration. We further investigated the function of Fas signaling in CRC lines depending on the culture mode as we incubated HCT116 and HT29 cells with anti-FasR agonistic antibodies. It appeared to act in a line-dependent and culture mode-dependent manner and influenced some particular features of CSCs such as spherogenicity, proliferation and phenotype. Additionally, the analysis of mRNA level showed that disease progression is associated with significantly increased expression of FasR and/or FasL. In conclusion, our observation seems to confirm that spherical model of cancer lines is more reliable for some sophisticated analysis because of their greater resemblance to the CSCs from human CRC samples in comparison to commonly used adherent cells, at least according to aspects

of their biology analyzed in this study. That can be extended to the resemblance of *in vitro* sphere forming conditions to the *in vivo* environment. However, the greatest difference concerns the level of apoptosis, thus, this issue require further experiments.

## Introduction

The cancer stem cell (CSC) model is an attractive hypothesis that translates properties of normal stem cells into the cancer field, and explains some of the most lethal features of cancer. The CSC model proposes that the cells within the tumor are hierarchically organized and predicts the existence of the subpopulation of cells with high tumorigenicity that are able to both self-renew and to generate differentiated cancer cells (non-CSCs) (1,2). CSCs are thought also to be responsible for relapses of disease, sometimes years after chemo- or radiotherapy (3). Therefore, elucidating the mechanisms of CSC maintenance is important for understanding tumor cell persistence and relapses and may enable specific targeting of CSCs as a potential therapeutic strategy to stably eradicate cancer (4,5).

The most established pro-apoptotic activity of FasR (CD95, Apo-1) is to mediate the apoptosis of either virus-infected cells, useless/autoreactive T cells or cancer cells when engaged by a CD8<sup>+</sup> cytotoxic T lymphocytes (6). The fact that almost all known cancer cells express FasR, and the observation that the most cancer cells are resistant to apoptosis induction, suggests that stimulation of FasR may not be an effective approach to eliminate cancer cells comprising the main mass of tumor. In addition, stimulation of FasR could never be used in targeted therapy because of major side effects such as massive apoptosis induced in the liver (7).

FasR signaling has also been reported to have non-apoptotic activities (8,9), important, for example, for liver regeneration (10), migration of renal epithelial cells (11) and development of neurons (12,13). Functional evidence of a pro-survival function of FasR/FasL signaling in normal stem cells came from experiments which showed that the stimulation of FasR in neuronal stem cells did not cause cell death but rather increased cell survival. Additionally, deletion of

---

*Correspondence to:* Dr Magdalena Szaryńska, Department of Histology, Medical University of Gdansk, Debinki 1, 80-210 Gdansk, Poland  
E-mail: mszarynska@gumed.edu.pl

**Key words:** cancer stem cells, FasL, FasR, colorectal cancer

FasR resulted in reduced neurogenesis. Because cancer stem cells are supposed to originate from normal stem cells, FasR was found to gain pro-survival functions within tumors, improving growth, proliferation and invasion due to induction of cancer-associated signaling pathways such as: NF- $\kappa$ B and MAP-kinases (8,14,15).

The meaning of FasR/FasL signaling for CSC survival and maintenance of their specific features was the goal of experimental analysis conducted on various cancer cell lines, including colorectal, breast, ovarian, glioblastoma and renal cancer. The stimulation of FasR induced a conversion from non-CSCs to CSCs what was suggested to depend on retro-differentiation mechanism (16). Additionally, the inhibition of FasR activity with recombinant trimerized FasL (CD95L-T4) reduced cancer cell growth and metastasis after xenotransplantation of pancreatic ductal adenocarcinoma collected from 35 patients into a mouse model (17). The glioblastoma tumor cells collected from patients show the correlation between FasR expression and the presence of stem cell-like markers. FasR<sup>high</sup> cells revealed high self-renewal *in vitro* and high tumorigenic potential *in vivo* (18). CSCs were found to be almost completely resistant to CD95-mediated apoptosis and stimulation of FasR increased the number of CSCs and also prevented differentiation of these cells, suggesting that FasR expression on cancer cells maintains the CSC pool (6,16).

It has been shown that the expression of FasR/FasL in colorectal cancer (CRC) is associated with worse prognosis, metastasis and recurrence of disease (19-24). It has been presented that the elimination of either FasR or FasL cause the cancer cells to die (*in vitro* and *in vivo*) through a process termed as DICE (death induced by CD95 or CD95L elimination). DICE is a necrotic form of mitotic catastrophe characterized by cell swelling, ROS production causing DNA damage and activation of caspase-2 following mitochondrial outer membrane permabilization (6,25). The inhibition of DICE seems to be hardly possible because many different death pathways are induced. These observations suggest that DICE is a naturally occurring antitumor defense mechanism, which are able to eliminate cancer cells devoid of proper pro-apoptotic FasR/FasL signaling. The activity of FasR as a pro-survival factor seems to be mostly relevant to cancer stem cells, since cancer cells rarely or even never have mutated or deleted both alleles of FasR. Additionally, such potential therapeutic strategy seems to be safe since it was shown that none of the normal tissues during embryonic development in FASR/FASL-knockout mice showed growth defects or signs of cell death (6,25).

It is well accepted that spheroid cultures preserve more faithfully the characteristics of original tumor, including gene expression profiles, cellular heterogeneity, morphology and distribution depending on the access to oxygen, nutrients and growth factors, in comparison to adherent cultures (26). Spheroids mirror more reliably the three dimensional cellular context and relevant pathophysiological gradients of *in vivo* tumor, however, to which extent sphere formation assays favor the enrichment of CSCs is not fully clear yet. Spheres contain also differentiated/differentiating tumor cells which after leaving the original sphere cannot survive in *in vitro* environment and undergo anoikis related to cessation of epithelial-like adhering properties.

Importantly, most of the studies demonstrating CSC properties expanded in a spherical form were conducted on cancer cell lines of different origin, for example breast, lung, ovarian and colon (26-31). Most of our attempts to characterize spheroid cultures derived from fresh surgical CRC specimens and to compare them with commercially available CRC lines (HCT116 and HT29) seem to be very advantageous. In our study we focused on the analysis of the presence of both Fas ligand and its receptor on CRC stem cells in two cell lines: HCT116 and HT29, which appeared to be very useful for analyzing the resemblance of *in vitro* settings to *in vivo* environment after we modified their expansion model to SC-promoting. We wished to determine the relationships between the expression of FASR/FASL and other CSC features crucial/necessary for CRC stem cell success. Moreover, we also examined the general expression of both proteins in CRC samples to find the relationships between FASR/FASL mRNA level and the disease progression level. We hoped to add to the knowledge concerning the usefulness of cancer cell lines for chemotherapeutics activity/effectiveness analysis for potential clinical applications. FasR/FasL activity is still highly controversial since it is suspected to be engaged in the regulation of apoptosis, senescence and survival depending on the entire niche environment (6,15,32). Further studies are, however, needed to clarify the detailed signaling relationships between proteins from FasR/FasL-induced pathways.

## Materials and methods

All human samples used in the scope of this study were donated freely and written informed consent was obtained from the donor for the use of its sample in particular research part. Ethics approval was obtained from The Independent Bioethics Commission for Research of the Medical University of Gdansk.

*Isolation and expansion of CRC primary cell lines.* Freshly resected colon tumor tissue from 20 CRC patients from Department of General, Endocrine and Transplant Surgery, Medical University of Gdansk, Invasive Medicine Centre, Gdansk, Poland was collected and immediately processed in culture. All experimental chemicals were purchased from Sigma-Aldrich, Poznan, Poland, except for growth factors, which were purchased from R&D Systems, Biokom, Warszawa, Poland. Tissues were washed several times in serum-free Dulbecco's modified Eagle's medium (DMEM)-F12 supplemented with antibiotic-antimycotic agent. The specimens were minced into 1-2-mm<sup>3</sup> pieces followed by incubation in collagenase (20 ng/ml) and hyaluronidase (20 ng/ml) for 1.5 h at 37°C. Single cell suspension was obtained by mixing every 15 min and by filtration through a 70- $\mu$ m cell strainer. Primary colon spheroid culture (SC) were maintained in serum-free stem cell medium containing DMEM-F12 supplemented with ITS Liquid Media Complement (1X), BSA (4 mg/ml), glucose (3 ml/ml), HEPES (5 mM), L-glutamine (2 nM), progesterone (20 nM), putrescine (9.6  $\mu$ g/ml), heparin (4  $\mu$ mg/ml), EGF (20 ng/ml), bFGF (20 ng/ml), and antibiotic-antimycotic solution (1X). This medium will further be referred to as stem cell medium (SCM). For the need of this study, we used only early passaged SCs for analysis.

*Expansion of HCT116 and HT29 cell lines in adherent and spheroid cultures.* The HT29 and HCT116 human colon adenocarcinoma cell lines [obtained originally from the American Type Culture Collection (ATCC), Manassas, VA, USA] were employed in this study. The cells were cultured routinely as a monolayer in Dulbecco's modified Eagle's medium (DMEM), supplemented with 10% fetal bovine serum and 1% penicillin-streptomycin and 2 mM L-glutamine and incubated at 37°C under a humidified atmosphere of 5% CO<sub>2</sub>. The cells were serially subcultured by trypsin treatment when they achieved 80% confluency and the medium was renewed 2-3 times/week.

For the culture of spheroid forms of HCT116 and HT29 cell lines, they were grown in SCM characterized as indicated above. These cultures were maintained under these conditions for 5-6 passages before being used for experiments.

*Cell death assay (7AAD).* For cell death evaluation the 7AAD Via Probe (BD Biosciences, USA) was used. After adding 10 μm of Via Probe samples were incubated for 30 min, washed and resuspended in PBS prior to cytometric analysis.

*Flow cytometric analysis of cell phenotype.* CRC lines and cells separated from human tumor fragments were stained with the following cocktail of monoclonal antibodies purchased from BD Biosciences: anti-CD29-APC (clone MAR4, IgG1κ), anti-CD44-FITC (clone C26, IgG2bκ), anti-CD95-PE (clone DX2, C3H/Bi IgG1κ), anti-FasL Biotin (clone NOK-1, IgG1) coupled with streptavidin-APC. Anti-CD133/2-PE (clone 293C3, IgG2bκ) monoclonal antibodies were purchased from Miltenyi Biotec. After 30-min incubation in the dark, samples were fixed with 1% PFA on ice and prepared for further analysis. Flow cytometric analysis was performed using FACSCalibur flow cytometer (BD Biosciences).

*Measurements of cytokine concentrations.* The level of soluble FasL was analyzed in supernatants from cultures of CRC lines and CSCs isolated from CRC patient tissues using BD Cytometric Bead Array Flex Set system kits (BD Biosciences) according to the manufacturer's instructions. Briefly, capture beads were transferred into all tubes and samples were incubated for 1 h at RT. Afterwards, PE detection reagent was added to all tubes, which were incubated for 2 h at RT. The captured beads, detection reagent (reporter antibodies) and samples were incubated together to form sandwich complexes. After double washing the samples were resuspended in washing buffer and analyzed in a flow cytometer. Fluorescence intensity was proportional to the amount of a given cytokine in a vial and estimated according to the standard curves acquired after analysis of standard dilutions. Data from cytometric analysis were transformed into graphical and tabular formats using FCAP Array Software. Finally, results were presented as pg/ml.

*Analysis of apoptosis.* Levels of cell apoptosis were measured using an Annexin V-FITC Apoptosis Detection Kit™ (BD Biosciences), according to the manufacturer's instructions. Briefly, 5x10<sup>5</sup> cells were suspended in a staining mixture comprised of 100 μl binding buffer, 5 μl Annexin V-FITC and 5 μl propidium iodide. After 15-min incubation in RT,

in the dark, samples were diluted in binding buffer and prepared for further analysis. Flow cytometric analysis was performed within 30 min using FACSCalibur flow cytometer (BD Biosciences).

*Incubation of cells with anti-FasR antibodies.* Cells were seeded into the wells and stimulated with the usage of anti-FasR (BD, IgM, clone EOS9.1) or concomitant control antibodies (Thermo Fisher Scientific) in the concentration of 200 ng/ml. The medium was replaced every 2-3 days to keep the concentration of antibodies at equally high level. After 14 days of the culture the cells were analysed.

*Quantification of sphere sizes.* Analysis of sphere sizes obtained from cells cultured in sphere-forming media after 2 weeks of continuous treatment with either anti-FasR monoclonal antibodies or IgM control antibodies with the using of inverted microscope Olympus-CKX53 coupled with digital camera Olympus SC50. At least 50 spheres of each experimental option were measured.

*Material used for real-time PCR.* The specimens were obtained from Department of General, Endocrine and Transplant Surgery, Medical University of Gdansk, Invasive Medicine Centre, Gdansk, Poland and Department of Hepatology and Gastroenterology, Faculty of Medicine, Medical University of Gdansk, Poland from 2012 to 2014. Clinical data were collected at the time of enrollment (Table II). The study included 65 patients with CRC; 32 males and 33 females (mean age ± SD 68.1±11.8; range, 31-91 years). The exclusion criteria were: development of a second neoplastic disease, previous chemo- and/or radiotherapy, tumors located in anal canal and anus. The control group comprised 20 healthy subjects, 7 males and 13 females (mean age 57±14.2; range, 21-76 years) who underwent colonoscopy as a part of a routine screening for CRC. None of the sample donors suffered from inflammatory bowel disease, had a family history of CRC or were taking medications.

All steps regarding sample collection and proceeding were previously described (33). Briefly, CRC samples were obtained during surgical hemicolectomy (5x5x5 mm), whereas control group specimens were collected during colonoscopy (2x2x2 mm). Collected material was divided for histopathologic examination and molecular studies and tissues were processed within 20 min. after tumor resection. In control patients, one biopsy (2x2x2 mm) was fixed in 10% buffered neutral formalin for routine histological examination, whereas two specimens from the nearest location were collected for nucleic acid analyzes. Both tumor samples and mucosal biopsies were immediately placed in sterile vials containing RNAlater (Ambion-Life Technologies, Grand Island, NY, USA), left for 6 h at 4°C and then stored at -25°C until further analyses.

*Nucleic acids extraction and reverse transcription.* Total RNA was extracted from part of tumor samples (3x5x5 mm) and whole-sized mucosal biopsies of control patients using Total RNA kit (A&A Biotechnology, Gdynia, Poland) according to the manufacturer's protocol. Isolated RNA was quantified by spectrophotometry (Nanodrop ND 1000; Thermo Fisher

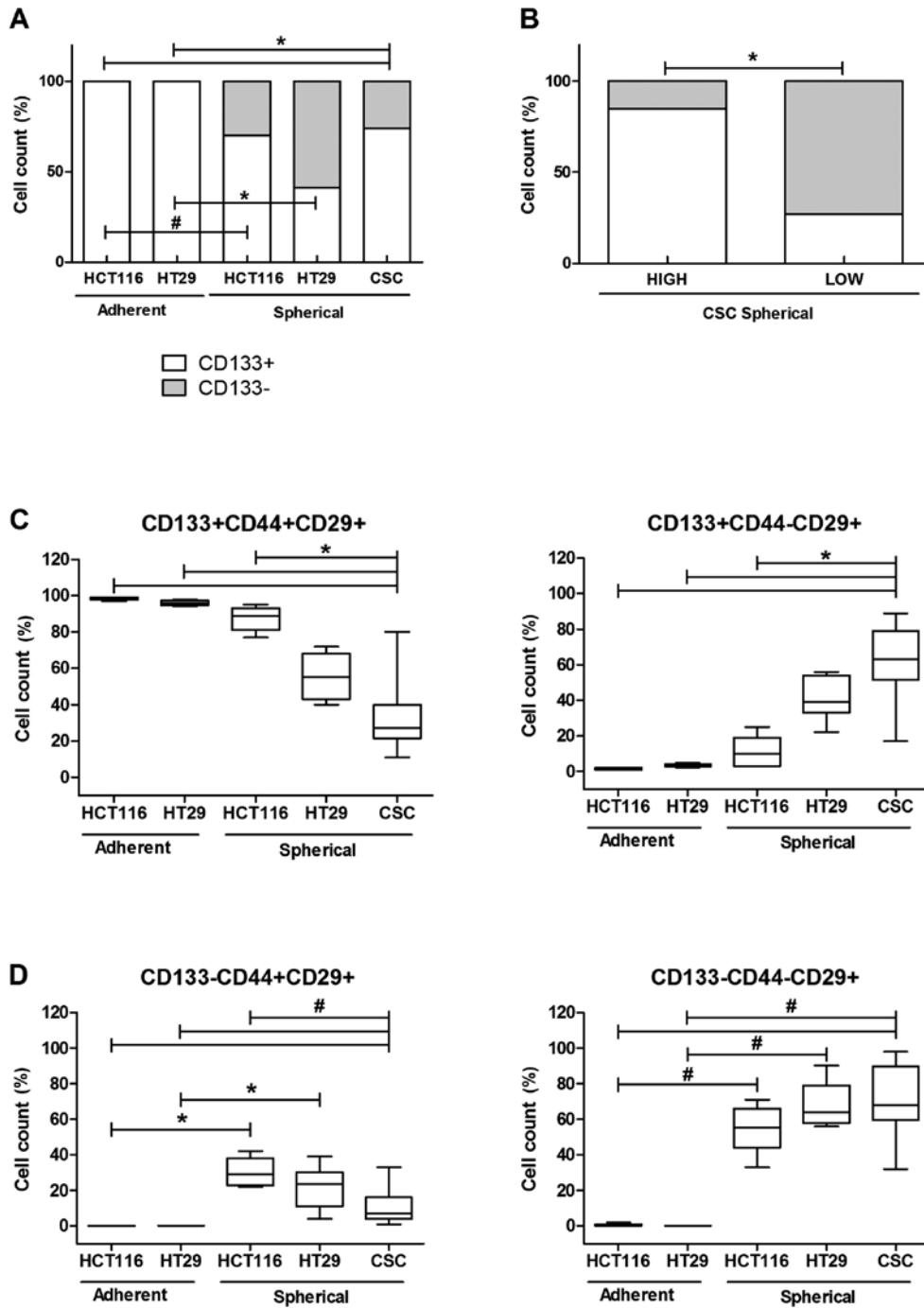


Figure 1. The phenotype of HCT116 and HT29 cells expanded in adherent and spherical form (n=14 for each cell population) and cancer cells isolated from human CRC fragments (n=20). y-axis presents cells of the given phenotype frequency (%). Bars and whiskers represent mean ± SEM (\* or #, statistical significance p<0.001 and p<0.05, respectively; ANOVA Kruskal-Wallis test). (A) The count of cells according to the presence of CD133 marker on their surface. (B) The count of cells from patient samples divided according to the average value of CD133<sup>+</sup> cell proportion (64%). (C and D) Detailed phenotypic analysis of all experimental sets.

Scientific, Fitchburg, WI, USA). DNA was digested with RNase-free DNase I (Fermentas; Thermo Fischer Scientific, Fitchburg, WI, USA) for 30 min at 37°C; afterwards DNase was inactivated by addition of EDTA and incubation at 65°C for 10 min. Before storing at -85°C, RNA integrity was analyzed by agarose gel electrophoresis. Total RNA (2 µg) were reverse-transcribed using 0.5 µg oligo(dT)18 primers (Sigma-Aldrich, Munich, Germany) and 200 U of RevertAid M-MuLV Reverse Transcriptase (Fermentas; Thermo Fischer

Scientific) in a total volume of 20 µl and resulting cDNA was stored at -25°C.

*Quantitative PCR assay for FASL and FASR mRNA level.* Quantification of FASL and FASR gene expression was carried out using StepOne Plus (Applied Biosystems, CA, USA) with SYBR® Green I as a fluorophore. FASL and FASR expression rates were determined by the comparative method 2<sup>-ΔΔCT</sup> (34) in relation to the geometric mean of the expression level of

PGK1 gene (normalization study results have not been published yet). QPCR conditions were validated, showing 90-100% efficiency for all assays. The amplification primer pairs were: 5'-GTTGACCGAATCACCGACCTCTC and 5'-AGAACAGAACATCCTTGCCAGC for PGK1, 5'-TTCCACCTACAGAAGGAGCTGGC and 5'-AGGTGTCTTCCCATTCCAGAGGC for FASL, 5'-GTGAACACTGTGACCCTTGCACC and 5'-CCTCTTTGCACTTGGTGTGCTG for FASR, respectively.

The reaction mixture (15  $\mu$ l) included 0.15  $\mu$ l of four times diluted reverse transcription product (cDNA), 0.2  $\mu$ M forward and reverse primers each, and SensiFast NoRoX SYBR Green (with EvaGreen fluorophore) (BioLine, London, UK). All reactions were performed in duplicate. For the studied genes the amplification profile was: 300-sec denaturation at 95°C, followed by 38 cycles of 5-sec denaturation at 95°C, 10 sec annealing at 58°C for 10 sec, elongation at 72°C for 15 sec and 5 sec fluorescence reading at 77-80°C. Dynamic melt curve analysis was applied to all reactions. Data were automatically collected and analyzed by StepOne Plus software ver. 2.2 (Applied Biosystems).

**Statistical analysis.** All data obtained during the study were analyzed with the use of GraphPad Prism ver. 6.05 (GraphPad Software, San Diego, CA, USA) and the software Statistica 12 (Statsoft, Poland) according to some non-parametric tests: U Mann-Whitney, Kruskal-Wallis ANOVA, Fisher's 2x2 exact test, Spearman's correlation. Values of  $p < 0.05$  were considered as statistically significant. The results are presented as average value  $\pm$  SD.

## Results

**Cytometric analysis of CRC cells.** We evaluated the CSC enrichment of CRC lines cultured under two distinct modes: spherical and adherent with the use of cytometric analysis of commonly used stem cell surface markers. We could observe that the adherent HCT116 and HT29 lines contained 100% of CD133<sup>+</sup> cells, whereas the conversion of culture conditions from adhering into sphere-forming was accompanied by the decrease of the CD133<sup>+</sup> cell proportion to 70 $\pm$ 11 and 41 $\pm$ 4% for mentioned CRC lines, respectively. Our analysis revealed that spherical HT29 cells presented higher content of CD133<sup>+</sup> cells in comparison to HCT116 line. Generally, adherent cells were more enriched in CD133<sup>+</sup>CD44<sup>+</sup>CD29<sup>+</sup> CSCs, whereas their spherical counterparts presented major heterogeneity, so HCT116 contained more CD133<sup>+</sup>CD44<sup>+</sup>CD29<sup>+</sup> (61 $\pm$ 8%) and HT29<sup>+</sup> more CD133<sup>+</sup>CD44<sup>+</sup>CD29<sup>+</sup> (41 $\pm$ 8) in general populations (Fig. 1). Additionally, adherent CRC lines (HCT116 and HT29) presented higher proportion of cells carrying FasR and FasL on their surface in comparison to their spherical counterparts (Fig. 2).

Because of high diversity of patient-derived spherical cultures, which appeared to contain varying proportion of CD133<sup>+</sup> cells (ranging from 9 to 98%), we divided our samples according to CD133 average number (average value was 64%) into 2 groups: with high (85 $\pm$ 10%) and low (28 $\pm$ 1.4%) CD133<sup>+</sup> cells proportions. We found these groups significantly different (Fig. 1B). Further analysis indicated the strong correlation between the time of their survival *in vitro*

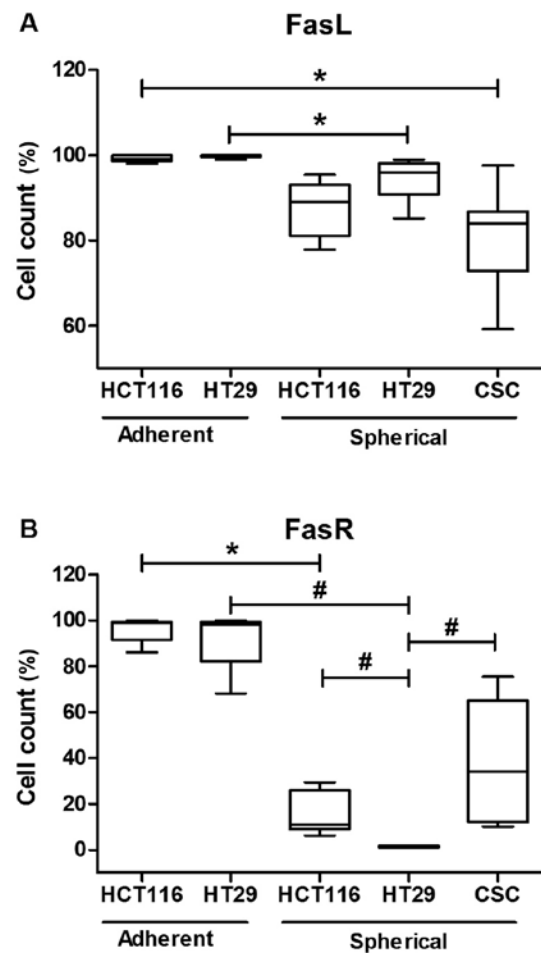


Figure 2. The analysis of FasL (A) and FasR (B) presence on the surface of HCT116 and HT29 cells expanded in adherent and spherical form (n=14 for each cell population) and cancer cells isolated from human CRC fragments (n=20). y-axis presents cells of the given phenotype frequency (%). Bars and whiskers represent mean  $\pm$  SEM (\* or #, statistical significance  $p < 0.001$  and  $p < 0.05$ , respectively; ANOVA Kruskal-Wallis test).

( $R=0.9$ ) and the number of CD133<sup>+</sup> cells. The cells expanded *in vitro* for at least 5 passages revealed to be highly enriched in CD133<sup>+</sup> cells in contrast to short-lasting expansions ( $p < 0.001$ , Kruskal-Wallis ANOVA) which we could maintain only for 2-4 days *in vitro*.

It has been shown that FasL can be found in two different forms: a membrane-bound (mFasL) and a soluble form (sFasL) that is generated through cleavage of mFasL by metalloproteinases (35). To test that issue in our experimental settings, we evaluated the presence of sFasL in tumor conditioned media from tumor cells expanded *in vitro* of both CRC lines and patient-derived samples. Surprisingly, we found that none of the analyzed cell populations released soluble FasL, whereas control leukocytes released up to 120 pg/ml of sFasL, representing unambiguous proof of methodology effectiveness.

**The cytometric analysis of cell death and/or apoptosis.** Because the Fas signaling in its canonical form is pro-apoptotic, we decided to correlate the dying/apoptosis rate with all previously presented parameters. The proportion of dying/apoptotic cells was assessed with the use of flow cytometric methodology utilizing different dyes: 7AAD and

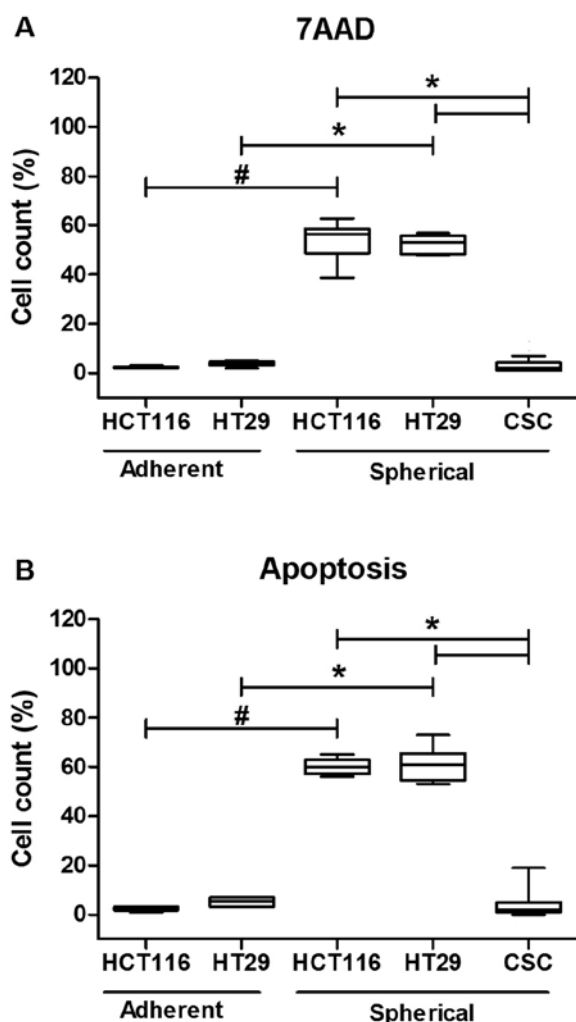


Figure 3. The cytometric analysis of cell viability during expansion of HCT116 and HT29 cells expanded in adherent and spherical forms (n=14 for each cell population) and cancer cells isolated from human CRC fragments (n=20). 7AAD dye (A) and Annexin V-FITC/PI (B) were used for staining dying or apoptotic cells. y-axis presents cells of the given phenotype frequency (%). Bars and whiskers represent mean  $\pm$  SEM (\* or #, statistical significance  $p < 0.001$  and  $p < 0.05$ , respectively; ANOVA Kruskal-Wallis test).

Annexin V-FITC/PI (Fig. 3). The cell death was quantified during each passage to test if it changed along the expansion time. Our analyses confirmed that HCT116 and HT29 cells expanded in adhering forms had much lower tendency for apoptosis as we found up to 5% of 7AAD<sup>+</sup> cells. The increase of both Annexin<sup>+</sup>/PI<sup>+</sup> and 7AAD<sup>+</sup> cell proportion during sphere-forming culture was ranging from 60 to 76%. Although, a substantial number of cells died, the overall cell number maintained at the same level or even slightly increased as we were measuring at each passage. Surprisingly, when we compared the CSC-enriched cultures derived from patient samples, we found that these cells were resistant to apoptosis thus the proportion of dying/apoptotic cells was very low and was ranging from 2 to 5% (Fig. 3). The number of patient-derived cells undergoing apoptosis was statistically significantly lower in comparison to HCT116 and HT-29-derived spherical cultures ( $p < 0.001$ , Kruskal-Wallis ANOVA). We found some significant correlations between the proportion of cancer cells CD29<sup>+</sup> and the proportion of

Table I. Correlations between the proportion of cells carrying different surface markers measured during each passage of spherical cells of both CRC lines (HCT116, HT29, n=14 for each line) and cells from CRC patients (n=11) (Spearman's rank correlation coefficients,  $p < 0.05$ ).

Correlated markers $p < 0.05$	R-values	p-values
<b>FasR</b>		
CD133	0.8	0.001
CD44	0.7	0.001
CD29	-0.8	0.0191
<b>FasL</b>		
CD133	0.3	0.0351
CD44	0.46	0.0020
CD29	0.6	0.001
<b>7AAD</b>		
CD133	-0.6	0.001
CD44	0.0	0.87
CD29	0.9	0.001
FasR	-0.7	0.001
FasL	0.3	0.0280

dying cells during expansion in all experimental sets, the highest correlation was observed for SC ( $R = 0.8$ ) (Table I). At the same time, the presence of FasR significantly negatively correlated with CD29<sup>+</sup> cancer cells ( $R = -0.8$ ) (Table I).

*The analysis of cells after incubation with anti-FasR antibodies.* After we exposed cancer lines to anti-FasR agonistic antibodies which were supposed to activate canonical apoptotic signaling, we expected this treatment would significantly eradicate FasR<sup>+</sup> cells in particular culture type. However, along the incubation time of adherent cells, according to the analysis conducted at each passage, we found that anti-FasR stimulation did not induce any significant differences concerning phenotype except the higher proportion of CD133<sup>+</sup>CD44<sup>+</sup>CD29<sup>+</sup> cells in comparison to control cells (Fig. 4B). The analysis of apoptosis rate did not show either any significant influence of such incubation (Fig. 5). Despite the lack of major phenotypic differences the anti-Fas stimulation seemed to inhibit the proliferation of both CRC cell lines in the adherent form (Fig. 6A).

When we examined the features of SCs we observed that HCT116 and HT29 cells behaved in distinct, line-specific way. Although we found that such prolonged FasR stimulation resulted in expansion of CD133<sup>+</sup> cells during SCs, the only difference for HCT116 was statistically significant. Moreover, the detailed phenotypic analysis presented altered number of cells bearing other CSC-like markers nevertheless the change had opposite direction for the cell lines (Fig. 4B and C). HT29 cells answered more effectively to our stimulation since the proportion of specific cell populations significantly changed. Additionally, anti-FasR treatment seemed to preferentially

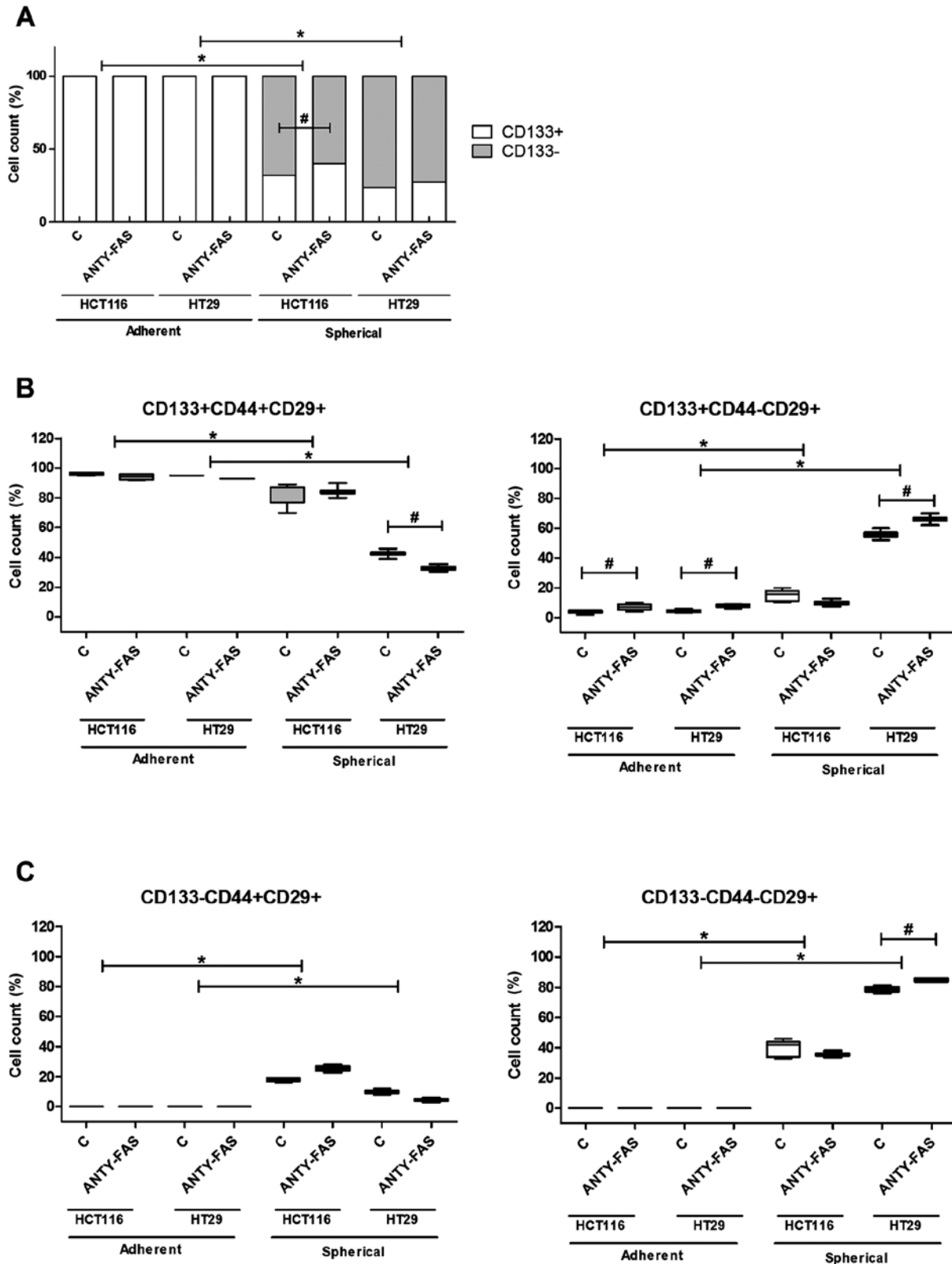


Figure 4. The phenotypic analysis of HCT116 and HT29 cells expanded 2 weeks in adherent and spherical forms with IgM control or with anti-FasR antibodies. (A) The count of cells according to the presence of CD133 marker on their surface. (B) Detailed phenotypic analysis of all experimental sets. Triplicate independent experiments were performed. Bars and whiskers represent mean  $\pm$  SEM (\* or #, statistical significance  $p < 0.001$  and  $p < 0.05$ , respectively; ANOVA Kruskal-Wallis test).

influence CD44<sup>+</sup> cells since the lowered count of these cells among both CD133<sup>+</sup> and CD133<sup>-</sup> was observed. Using flow cytometry to analyze dying cells we confirmed that the

anti-FasR antibodies could not influence the apoptosis susceptibility of cells during SCs. At the same time such stimulation increased spherogenicity of CRC cells as the significantly

Table II. Clinicopathological characteristics of CRC patients included into the real-time PCR analysis of *FASL* and *FASR* mRNA levels.

CRC patients, n=65 Control, n=20	Subgroups	FASL n (% of all CRC patients)			FASR n (% of all CRC patients)		
		Low ( $\leq 0.985$ )	High ( $> 0.985$ )	P-value <sup>b</sup>	Low ( $\leq 2.99$ )	High ( $> 2.99$ )	P-value <sup>b</sup>
Age (years)	$\leq 68$ n=26	5 (8)	21 (32)	0.39	15 (23)	11 (17)	0.40
68.1 $\pm$ 11.06 (Mean $\pm$ SD) Range, 31-91	$> 68$ n=39	10 (15)	29 (45)		20 (31)	19 (29)	
Sex	Female n=33	8 (12)	25 (38)	1.00	18 (18)	15 (23)	1.00
	Male n=32	7 (11)	25 (38)		17 (26)	15 (23)	
Tumor size (cm)	$\leq 5$ cm n=39	12 (18)	27 (42)	0.08	23 (35)	16 (25)	0.32
	$> 5$ cm n=26	3 (5)	23 (35)		12 (18)	14 (22)	
Histological differentiation G stage	G2 n=50	13 (21)	37 (61)	0.43	28 (46)	22 (36)	0.73
	G3 n=11	1 (2)	10 (16)		5 (8)	6 (10)	
TNM stages							
Non-metastatic	TNM I $\pm$ II n=34	6 (9)	28 (43)	0.38	17 (26)	17 (26)	0.62
Metastatic	TNM III $\pm$ IV n=31	9 (14)	22 (34)		18 (28)	13 (20)	

<sup>a</sup>The comparison of *FASR/FASL* mRNA expression between groups of patients divided according to the used threshold based on the median mRNA ratios of either *FASL* or *FASR* in control groups (low versus high). <sup>b</sup>p-values were calculated by Fisher's 2x2 test between groups referred as low versus high.

increased spheres were found in comparison to control culture (Fig. 6B).

*The expression of the FASL and FASR genes at the mRNA level.* As shown in Fig. 7A, the *FASL* mRNA expression ratio was approximately 80 times higher in tumor CRC samples in comparison to level in 20 biopsies taken from control group of non-CRC patients. Although we observed a tendency for elevated mRNA ratio of *FASR* gene in tumor samples, the difference was not statistically significant (Fig. 7B). When mRNA median ratios of either *FASL* or *FASR* in control groups were taken into consideration as the threshold, we found that 50 of 65 tumor CRC samples shown increased *FASL* mRNA content; for *FASR* such difference was not statistically significant (in 30 samples we found increased and in 35 decreased *FASR* mRNA ratio, Table II). Interestingly, we observed positive correlation between mRNA levels of *FASL* and *FASR* in tumor samples of CRC patients ( $R = 0.54$ ,  $p < 0.05$ , Fig. 8).

Furthermore, regarding the clinicopathological data, we found that patients with advanced CRC (TNM stages III and IV) were characterized by  $\sim 10$ -fold increased *FASL* mRNA content in comparison to patients with early CRC (TNM stages I and II, Fig. 1C). We found no statistically significant differences between the expression of *FASR* in biopsies from CRC in I and II TNM stages in comparison to samples collected from CRC patients in III and IV stages. When we compared the data to the *FASR* expression in healthy tissue we also found no significant difference.

## Discussion

Colorectal cancer is one of the most common solid organ cancers prevalent worldwide causing, in spite of advances in therapeutic methodology, high rate of patient mortality, especially due to metastasis development. The cancer stem cell theory of tumor growth indicates that CSCs within the tumor mass have great capacity to initiate and sustain tumor growth.



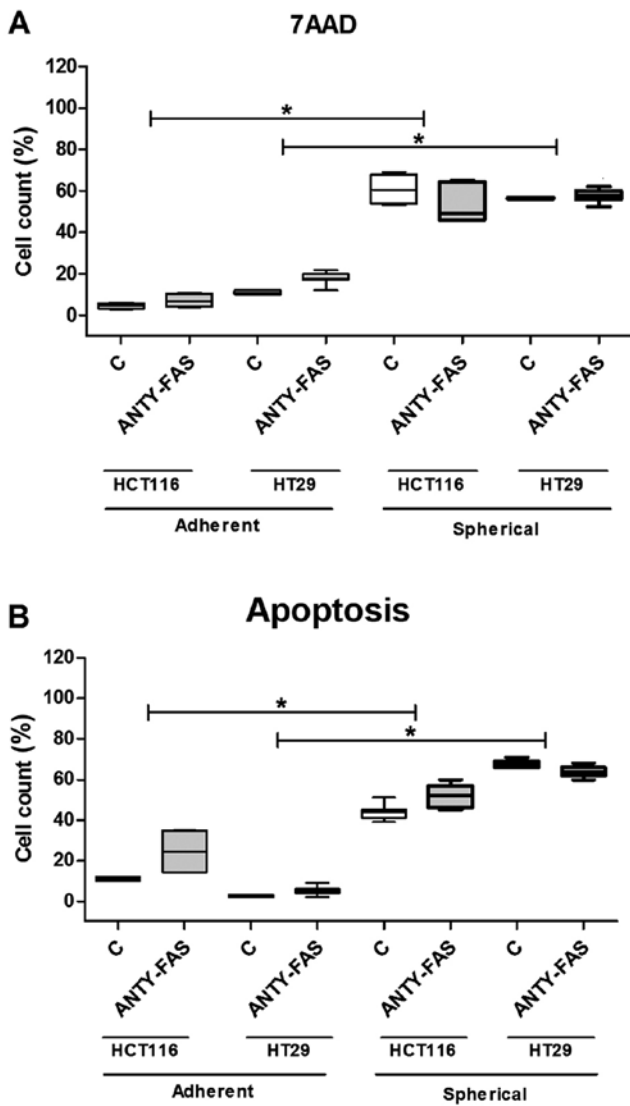


Figure 5. The cytometric analysis of HCT116 and HT29 cell viability during 2-week expansion with IgM control or with anti-FasR antibodies. 7AAD dye (A) and Annexin V-FITC/PI (B) were used for staining dying or apoptotic cells. Triplicate independent experiments were performed. y-axis presents cells of the given phenotype frequency (%). Bars and whiskers represent mean  $\pm$  SEM (\* or #, statistical significance  $p < 0.001$  and  $p < 0.05$ , respectively; ANOVA Kruskal-Wallis test).

According to current state of knowledge, CSCs are said to be responsible for metastasis, recurrence, relapse and resistance to conventional chemotherapy. Taking all these pessimistic facts the CSC biology decipherment seems to be necessary to find some new efficient therapeutic strategies (36).

The crucial role of FasR/FasL signaling for the regulating of cancer cell death/fate has been revealed recently since it was associated with not only pro-apoptotic pathways but also with some death-independent activities. Despite the canonical apoptotic pathway is well described, the signaling of opposite activities is less understood. Especially DICE (death induced by CD95 or CD95L elimination) deserves special attention, as it seems to be a unique protecting mechanism of immune system against cancer cells devoid of FasR (6). Conversion of non-CSCs into CSCs resulted in a loss of sensitivity to Fas-mediated apoptosis and a concomitant increase in the

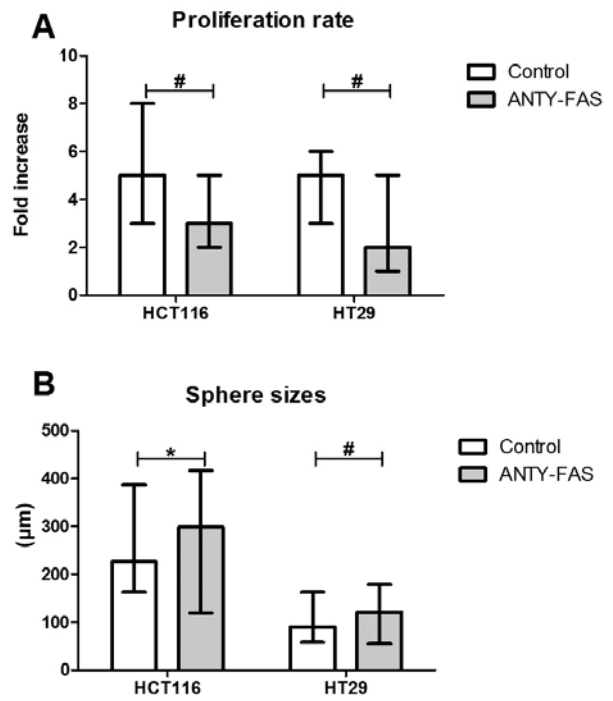


Figure 6. Analysis of HCT116 and HT29 cells during 2-week expansion with IgM control or with anti-FasR antibodies (n=3 for each cell population). (A) Proliferation rate of cells during adherent culture evaluated during each passage based on the cell number. (B) Sphere sizes measured during each passage. At least 50 spheres of each experimental option were measured. Bars and whiskers represent mean  $\pm$  SEM (\* or #, statistical significance  $p < 0.001$  and  $p < 0.05$ , respectively; ANOVA Kruskal-Wallis test).

sensitivity of cells to DICE (16). In fact, DICE was found to preferentially target CSCs demonstrating that HCT116 cells with the use of tetracycline analog (Dox) knocked down FasR and decreased the spherogenicity (16). Similar results were achieved with the human breast cancer MCF7 and T4F7, ovarian cancer HeyA8 and mouse colon cancer CT26L cell lines (16,25). When DICE was induced in the mentioned cancer cell lines, the number of CSCs and effectiveness of sphere formation were lowered and finally CSCs became depleted from experimental populations (37).

In this study we demonstrated that the level of FasR was significantly reduced in cells cultured under sphere-forming conditions in comparison to cells expanded in adherent form of both examined cell lines. This observation suggested that the decreasing of FasR level (96 to 16% for HCT116 and 92 to 1% for HT29) (Fig. 1) must have the association with the culture mode and higher diversity of cells since the strong ( $R=0.8$ ) correlation between CD133 and FasR was found. Moreover, the lower level of FasR in SCs seemed to confirm the higher resemblance of 3D culture system to *in vivo* environment of tumor development. CSC maintenance depends on the presence of FasR on their surface at a minimal level sufficient to promote their optimal growth (6,9,16,25), although, the lower FasR proportion can be interpreted in the context of adaptation of cancer cells to co-existence with immunological cells to reduce the risk of undergoing apoptosis while benefiting from tumorigenic activities.

We demonstrated that spherical forms of CRC lines diminished the level of FasL to similar level as CSCs isolated from tumor fragments of CRC patients (Fig. 1), although only for

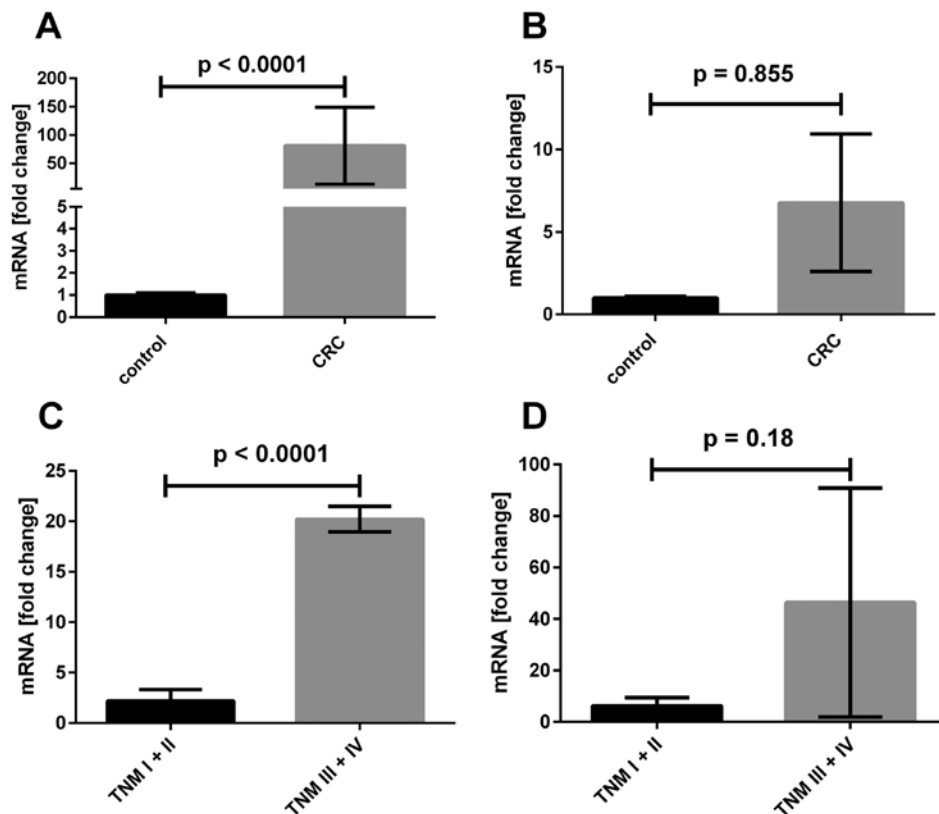


Figure 7. *FASL* and *FASR* gene expression in CRC samples in comparison to control group which is used as threshold ( $c=1$  value). *FASL* (A) and *FASR* (B) mRNA levels in tissue samples of CRC ( $n=65$ ) and control ( $n=20$ ) patients were assessed by qPCR. Plots (C) and (D) show gene expression in tumor samples related to TNM grading. Bars and whiskers represent mean  $\pm$  SEM normalized to control samples (U Mann-Whitney test,  $p < 0.05$ ).

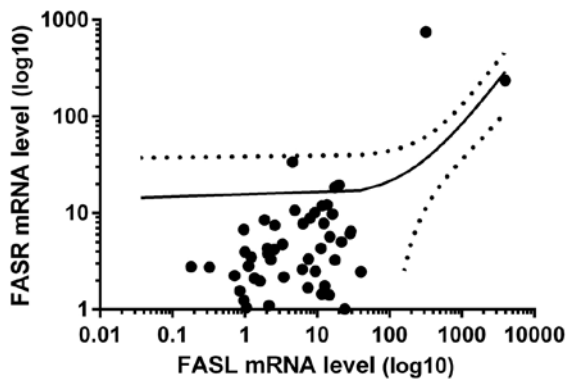


Figure 8. Correlation between mRNA levels of *FASL* and *FASR* in CRC samples ( $n=65$ ) (Spearman's rank correlation coefficients,  $p < 0.5$ ).

HT29 cells that change were statistically significant. FasL was described as a positive prognostic marker for colorectal carcinoma (19,20,22,38) and the vast majority of reports show that disease progression is associated with progressively increasing expression of FasL and/or FasR what seems to be in agreement with some of our results. Taking into consideration that HCT116 cells originate from a poorly differentiated (high-grade, more aggressive) colon cancer, whereas HT29 cell line is derived from well-differentiated (low-grade, less aggressive) CRC, the higher proportion of FasR<sup>+</sup> HCT116 cells in comparison to HT29 cells ( $15 \pm 9$  versus  $1 \pm 0.5$ , respectively) in their spherical forms seemed to confirm such attitude, whereas the analogous difference was not found

for FasL ( $87 \pm 6$  versus  $94 \pm 5$ , respectively). The analysis of *FASR/FASL* expression profiles showed their compatibility with our *in vitro* experimental data. The increased expression of both genes was found in tumor tissue in comparison to healthy control samples, however, only for *FASL* the difference reached statistically significant level. Additionally, depending on the progression status of CRC the elevated level of *FASR/FASL* expression was shown (Fig. 2). The samples collected from patients representing higher-grade tumor (TNM III and IV) indicated higher expression of both genes, but only for *FASL* this difference was statistically significant, however, *FASR* revealed substantial tendency.

The cytometric analysis of phenotype indicated some interesting relationships between measured protein markers on the surface of analyzed cell populations. Decreasing of the FasR and/or FasL was suggested to be associated with the elevating number of 7AAD-positively stained cells and decreasing of CD133<sup>+</sup>CD29<sup>+</sup>CD44<sup>+</sup> CSC proportion. The only exception were CD29<sup>+</sup> cells (CD29<sup>+</sup>CD133<sup>-</sup>CD44<sup>-</sup>) which proportion increased after the culture conditions were modified and that was accompanied by markedly increased apoptosis rate. We concluded that CD133 marker is indirectly associated with maintenance and higher proliferative properties of cells, and CD29<sup>-</sup> with higher differentiation and/or dying as we found the significant phenotypic correlations (Fig. 1 and Table I). Moreover, the level of CD133 and CD44 (Table I) strongly correlated with the presence of FasR on the SCs cell surface ( $R=0.7$  and  $R=0.8$ , respectively), whereas we could not find such correlations for adherent cells.

The phenotypic changes observed in our experimental settings suggested that the death type possessed some features of DICE because DICE was earlier demonstrated to preferentially target CSCs (6,16). We found significant decline of CD44<sup>+</sup> cells when expanded in spherical form in comparison to their adherent counterparts (Fig. 1) and lowered proportion of CD44<sup>+</sup> cells after blockade of the FasR by agonistic antibodies (Fig. 4). As previously shown (16), DICE is able to eliminate CD44<sup>+</sup> CSCs of breast cancer MCF-7 and T47D cells. We could observe during cytometric analysis that cells of the highest values of FSC and SSC parameters represented simultaneously cells with higher proportion of apoptosis (60 versus 85% for FSC<sup>low</sup>SSC<sup>low</sup> cells and FSC<sup>high</sup>SSC<sup>high</sup>, respectively, data not shown) this seemed to confirm the presence of swelling cells characteristic for DICE (6,25). Significant correlations were found between FasR and some CSC-like markers, which seem to indicate the cancer progression promoting role of FasR/FasL signaling, however the correlations for FasL were not so substantial (Table I).

We further investigated the function of Fas signaling in our CRC lines depending on the culture mode as we incubated HCT116 and HT29 cells with anti-FasR agonistic antibodies. We found that adherent cells only slightly answered to that stimulation (Figs. 4 and 5), except the markedly decreased proliferation rate (Fig. 6A). That seems to proof the engagement of FasR in the senescence induction accompanied by the cell cycle arrest as was suggested earlier by Raats *et al* (32). Surprisingly, the Raats group (32) correlated the presence of wild KRAS gene with FasR inhibitory effects. Although HCT116 cells are known to have mutated form of KRAS (according to ATCC specification) (39), they answered efficiently to anti-FasR antibodies during expansion. Thus the relationships between Fas signaling cytoplasmic effectors must be much more complex and require more efforts. The lower number of cells could not be linked to increased apoptosis as the cytometric analysis did not show any significant differences in comparison to control cells, anyway some minor tendencies could be seen (Fig. 5). The assessment of SCs revealed that the effects are cancer line-dependent and additionally the prolonged incubation with anti-FasR antibodies could induce different effects in comparison to these observed for adherent cells. We found that such FasR stimulation resulted in increased expansion of CD133<sup>+</sup> cells during SC indicating specific clonal selection of cells sensitive to Fas-mediated supporting stimulation. During SC with anti-Fas antibodies no substantial apoptosis rate increase was observed, similarly to data obtained during adherent cultures. Our results are in line with findings of other groups suggesting that the Fas pathway have rather pro-survival activity inducing growth, invasion and metastasis of cancer cells, especially CSCs (16,25,32,40). The increased sphere sizes following 2-week incubation with anti-FasR antibodies agreed with mentioned tumor-promoting activity of Fas signaling (Fig. 6B) because that feature might be directly associated with increased spherogenicity and, by extension-aggressiveness of tumor cells.

Recently it has been demonstrated that expression of FasL by apoptosis-resistant tumor cells enables a powerful 'counterattack' against antitumor immune effectors which are themselves sensitive to Fas-mediated apoptosis (41,42). However, while there is some evidence for the occurrence of

this counterattack, its existence remains controversial (6,41,43). The reported increased concentration of soluble FasL (sFasL) in the serum of many cancer patients was often interpreted in the context of the FasL counterattack theory and would suggest a possible immunosuppressive role of this molecule. However, the generalized immune suppression that would be expected from this situation could not be confirmed in cancer patients; thus, perhaps the increased FasL expression in tumor tissues has a more direct tumor promoting role (6,41,43). The negative results concerning sFasL in media from over the expanded CRC cells from our experiments were surprising in this context; the more so because that was shown to be a prognostic factor for different types of cancers (44,45). The levels presented in the mentioned manuscripts (from 0.16-0.17 to 21 ng/ml) were much higher than the sensitivity level of our methodology which was 2.6 pg/ml therefore this issue needs deeper analysis.

In conclusion, FasR/FasL signaling as the target of CRC therapy is not utilized nowadays because of its toxic side effects especially observed in liver. Moreover, since DICE was suggested being a naturally-occurring antitumor defense mechanism, which enable elimination of CSCs devoid of FasR/FasL (6), it is reasonable to broaden our knowledge concerning Fas-signaling and its cytoplasmic effectors. Our study hopefully enriched the knowledge concerning this issue. The next advantage of our study seems to be the comparison of different modes of expansion of cancer cell lines and contrast these data with information obtained from analysis of cancer cells separated from CRC patients. Our observation seems to confirm that spherical model of cancer lines is more reliable for some sophisticated analysis because of their greater resemblance to the CSCs from human CRC samples in comparison to commonly used adherent cells, at least according to aspects of their biology analyzed in this study, and can be extended to the resemblance of *in vitro* sphere forming conditions to the *in vivo* environment. However, the greatest difference concerns the level of apoptosis thus this issue require further experimental analysis.

## Acknowledgements

This study was supported by Polish Ministry of Science grants nos. N N402 684040 and N N402 683940.

## References

1. Reya T, Morrison SJ, Clarke MF and Weissman IL: Stem cells, cancer, and cancer stem cells. *Nature* 414: 105-111, 2001.
2. Charafe-Jauffret E, Ginestier C and Birnbaum D: Breast cancer stem cells: Tools and models to rely on. *BMC Cancer* 9: 202, 2009.
3. Creighton CJ, Li X, Landis M, Dixon JM, Neumeister VM, Sjolund A, Rimm DL, Wong H, Rodriguez A, Herschkowitz JI, *et al*: Residual breast cancers after conventional therapy display mesenchymal as well as tumor-initiating features. *Proc Natl Acad Sci USA* 106: 13820-13825, 2009.
4. Gupta PB, Chaffer CL and Weinberg RA: Cancer stem cells: Mirage or reality? *Nat Med* 15: 1010-1012, 2009.
5. Frank NY, Schatton T and Frank MH: The therapeutic promise of the cancer stem cell concept. *J Clin Invest* 120: 41-50, 2010.
6. Peter ME, Hadji A, Murmann AE, Brockway S, Putzbach W, Pattanayak A and Ceppi P: The role of CD95 and CD95 ligand in cancer. *Cell Death Differ* 22: 885-886, 2015.
7. Ogasawara J, Watanabe-Fukunaga R, Adachi M, Matsuzawa A, Kasugai T, Kitamura Y, Itoh N, Suda T and Nagata S: Lethal effect of the anti-Fas antibody in mice. *Nature* 364: 806-809, 1993.

8. Martin-Villalba A, Llorens-Bobadilla E and Wollny D: CD95 in cancer: Tool or target? *Trends Mol Med* 19: 329-335, 2013.
9. Chen L, Park SM, Tumanov AV, Hau A, Sawada K, Feig C, Turner JR, Fu YX, Romero IL, Lengyel E, *et al*: CD95 promotes tumour growth. *Nature* 465: 492-496, 2010.
10. Desbarats J and Newell MK: Fas engagement accelerates liver regeneration after partial hepatectomy. *Nat Med* 6: 920-923, 2000.
11. Jarad G, Wang B, Khan S, DeVore J, Miao H, Wu K, Nishimura SL, Wible BA, Konieczkowski M, Sedor JR, *et al*: Fas activation induces renal tubular epithelial cell beta 8 integrin expression and function in the absence of apoptosis. *J Biol Chem* 277: 47826-47833, 2002.
12. Desbarats J, Birge RB, Mimouni-Rongy M, Weinstein DE, Palerme JS and Newell MK: Fas engagement induces neurite growth through ERK activation and p35 upregulation. *Nat Cell Biol* 5: 118-125, 2003.
13. Zuliani C, Kleber S, Klussmann S, Wenger T, Kenzelmann M, Schreglmann N, Martinez A, del Rio JA, Soriano E, Vodrazka P, *et al*: Control of neuronal branching by the death receptor CD95 (Fas/Apo-1). *Cell Death Differ* 13: 31-40, 2006.
14. Corsini NS, Sancho-Martinez I, Laudenklos S, Glasgow D, Kumar S, Letellier E, Koch P, Teodorczyk M, Kleber S, Klussmann S, *et al*: The death receptor CD95 activates adult neural stem cells for working memory formation and brain repair. *Cell Stem Cell* 5: 178-190, 2009.
15. Siegmund D, Lang I and Wajant H: Cell death-independent activities of the death receptors CD95, TRAILR1, and TRAILR2. *FEBS J* 284: 1131-1159, 2017.
16. Ceppi P, Hadji A, Kohlhapp FJ, Pattanayak A, Hau A, Liu X, Liu H, Murmann AE and Peter ME: CD95 and CD95L promote and protect cancer stem cells. *Nat Commun* 5: 5238, 2014.
17. Teodorczyk M, Kleber S, Wollny D, Seifrin JP, Aykut B, Mateos A, Herhaus P, Sancho-Martinez I, Hill O, Gieffers C, *et al*: CD95 promotes metastatic spread via Sck in pancreatic ductal adenocarcinoma. *Cell Death Differ* 22: 1192-1202, 2015.
18. Drachler M, Kleber S, Mateos A, Volk K, Mohr N, Chen S, Cirovic B, Tüttenberg J, Gieffers C, Sykora J, *et al*: CD95 maintains stem cell-like and non-classical EMT programs in primary human glioblastoma cells. *Cell Death Dis* 7: e2209, 2016.
19. Li H, Fan X, Stoicov C, Liu JH, Zubair S, Tsai E, Ste Marie R, Wang TC, Lyle S, Kurt-Jones E, *et al*: Human and mouse colon cancer utilizes CD95 signaling for local growth and metastatic spread to liver. *Gastroenterology* 137: 934-944, 944.e931-934, 2009.
20. Hoogwater FJ, Nijkamp MW, Smakman N, Steller EJ, Emmink BL, Westendorp BF, Raats DA, Sprick MR, Schaefer U, Van Houdt WJ, *et al*: Oncogenic K-Ras turns death receptors into metastasis-promoting receptors in human and mouse colorectal cancer cells. *Gastroenterology* 138: 2357-2367, 2010.
21. Kykalos S, Mathaiou S, Karayiannakis AJ, Patsouras D, Lambropoulou M and Simopoulos C: Tissue expression of the proteins fas and fas ligand in colorectal cancer and liver metastases. *J Gastrointest Cancer* 43: 224-228, 2012.
22. Nijkamp MW, Hoogwater FJ, Steller EJ, Westendorp BF, van der Meulen TA, Leenders MW, Borel Rinkes IH and Kranenburg O: CD95 is a key mediator of invasion and accelerated outgrowth of mouse colorectal liver metastases following radiofrequency ablation. *J Hepatol* 53: 1069-1077, 2010.
23. Sträter J, Hinz U, Hasel C, Bhanot U, Mechttersheimer G, Lehnert T and Möller P: Impaired CD95 expression predisposes for recurrence in curatively resected colon carcinoma: Clinical evidence for immunoselection and CD95L mediated control of minimal residual disease. *Gut* 54: 661-665, 2005.
24. Zhang W, Ding EX, Wang Q, Zhu DQ, He J, Li YL and Wang YH: Fas ligand expression in colon cancer: A possible mechanism of tumor immune privilege. *World J Gastroenterol* 11: 3632-3635, 2005.
25. Hadji A, Ceppi P, Murmann AE, Brockway S, Pattanayak A, Bhinder B, Hau A, De Chant S, Parimi V, Kolesza P, *et al*: Death induced by CD95 or CD95 ligand elimination. *Cell Rep* 7: 208-222, 2014.
26. Weiswald LB, Bellet D and Dangles-Marie V: Spherical cancer models in tumor biology. *Neoplasia* 17: 1-15, 2015.
27. Hirschhaeuser F, Menne H, Dittfeld C, West J, Mueller-Klieser W and Kunz-Schughart LA: Multicellular tumor spheroids: An underestimated tool is catching up again. *J Biotechnol* 148: 3-15, 2010.
28. Chandrasekaran S, Marshall JR, Messing JA, Hsu JW and King MR: TRAIL-mediated apoptosis in breast cancer cells cultured as 3D spheroids. *PLoS One* 9: e111487, 2014.
29. Endo H, Okami J, Okuyama H, Kumagai T, Uchida J, Kondo J, Takehara T, Nishizawa Y, Imamura F, Higashiyama M, *et al*: Spheroid culture of primary lung cancer cells with neuregulin 1/HER3 pathway activation. *J Thorac Oncol* 8: 131-139, 2013.
30. Tong JG, Valdes YR, Barrett JW, Bell JC, Stojdl D, McFadden G, McCart JA, DiMattia GE and Shepherd TG: Evidence for differential viral oncolytic efficacy in an in vitro model of epithelial ovarian cancer metastasis. *Mol Ther Oncolytics* 2: 15013, 2015.
31. Qureshi-Baig K, Ullmann P, Rodriguez R, Frascuelo S, Nazarov PV, Haan S and Letellier E: What do we learn from spheroid culture systems? Insights from tumorspheres derived from primary colon cancer tissue. *PLoS One* 11: e0146052, 2016.
32. Raats DA, Frenkel N, van Schelven SJ, Rinkes IH, Laoukili J and Kranenburg O: CD95 ligand induces senescence in mismatch repair-deficient human colon cancer via chronic caspase-mediated induction of DNA damage. *Cell Death Dis* 8: e2669, 2017.
33. Wierzbicki PM, Adrych K, Kartanowicz D, Stanislawowski M, Kowalczyk A, Godlewski J, Skwierz-Bogdanska I, Celinski K, Gach T, Kulig J, *et al*: Underexpression of LATS1 TSG in colorectal cancer is associated with promoter hypermethylation. *World J Gastroenterol* 19: 4363-4373, 2013.
34. Schmittgen TD and Livak KJ: Analyzing real-time PCR data by the comparative C(T) method. *Nat Protoc* 3: 1101-1108, 2008.
35. O'Reilly LAI, Tai L, Lee L, Kruse EA, Grabow S, Fairlie WD, Haynes NM, Tarlinton DM, Zhang JG, Belz GT, *et al*: Membrane-bound Fas ligand only is essential for Fas-induced apoptosis. *Nature* 461: 659-663, 2009.
36. Todaro M, Francipane MG, Medema JP and Stassi G: Colon cancer stem cells: Promise of targeted therapy. *Gastroenterology* 138: 2151-2162, 2010.
37. Schickel R, Park SM, Murmann AE and Peter ME: miR-200c regulates induction of apoptosis through CD95 by targeting FAP-1. *Mol Cell* 38: 908-915, 2010.
38. Steller EJ, Ritsma L, Raats DA, Hoogwater FJ, Emmink BL, Govaert KM, Laoukili J, Rinkes IH, van Rheejen J and Kranenburg O: The death receptor CD95 activates the cofilin pathway to stimulate tumour cell invasion. *EMBO Rep* 12: 931-937, 2011.
39. Hong S, Kim S, Kim HY, Kang M, Jang HH and Lee WS: Targeting the PI3K signaling pathway in KRAS mutant colon cancer. *Cancer Med* 5: 248-255, 2016.
40. Élez E, Kocáková I, Höhler T, Martens UM, Bokemeyer C, Van Cutsem E, Melichar B, Smakal M, Csósz T, Topuzov E, *et al*: Abituzumab combined with cetuximab plus irinotecan versus cetuximab plus irinotecan alone for patients with KRAS wild-type metastatic colorectal cancer: The randomised phase I/II POSEIDON trial. *Ann Oncol* 26: 132-140, 2015.
41. Igney FH and Krammer PH: Tumor counterattack: Fact or fiction? *Cancer Immunol Immunother* 54: 1127-1136, 2005.
42. O'Connell J, O'Sullivan GC, Collins JK and Shanahan F: The Fas counterattack: Fas-mediated T cell killing by colon cancer cells expressing Fas ligand. *J Exp Med* 184: 1075-1082, 1996.
43. Igney FH and Krammer PH: Death and anti-death: Tumour resistance to apoptosis. *Nat Rev Cancer* 2: 277-288, 2002.
44. Hoogwater FJ, Snoeren N, Nijkamp MW, Gunning AC, van Houdt WJ, DE Bruijn MT, Voest EE, van Hillegersberg R, Kranenburg O and Rinkes IH: Circulating CD95-ligand as a potential prognostic marker for recurrence in patients with synchronous colorectal liver metastases. *Anticancer Res* 31: 4507-4512, 2011.
45. Konno R, Takano T, Sato S and Yajima A: Serum soluble fas level as a prognostic factor in patients with gynecological malignancies. *Clin Cancer Res* 6: 3576-3580, 2000.